

Structure of epitaxial Gd_2O_3 films grown on GaAs(100)

A. R. Kortan, M. Hong, J. Kwo, J. P. Mannaerts, and N. Kopylov
Bell Laboratories, Lucent Technologies, Murray Hill, New Jersey 07974-0636

(Received 6 April 1999)

Single-crystal Gd_2O_3 films were grown epitaxially on GaAs(100) substrate. From the single-crystal momentum space analysis on four different samples, 185, 45, 25, and 18 Å thick, a Mn_2O_3 isomorphous cubic structure is identified. The Gd_2O_3 film aligns its twofold (110) axis with the fourfold (100) surface normal of the substrate, while aligning its [001] and $[\bar{1}10]$ axes with the [011] and $[01\bar{1}]$ axes of GaAs within the plane, respectively. The absence of the other possible twofold growth orientation can be explained by the bonding configuration at the interface. The 18- and 25-Å-thick samples show an elastically strained component in the film, while thicker samples appear fully relaxed, probably through misfit dislocation formation.
 [S0163-1829(99)08439-8]

I. INTRODUCTION

Reliable passivation layers on semiconductors are becoming increasingly more critical as the device sizes continuously decrease. In the case of silicon passivation, amorphous oxide layers have performed well in submicron devices. Smaller devices (on the order of 0.1 μm or less) require thinner oxide layer thickness, which is now approaching a dimension of several atomic layers. Limitations on the conventional oxide have prompted an intensive search for better gate dielectrics to be used in such a regime. Among them, a defect-free and thermodynamically stable single-crystal oxide film layer may best fulfill the requirements for such small transistors. For GaAs, a successful surface passivation remained as an unsolved key issue in compound semiconductor technology for the past three decades, until our discovery of an amorphous oxide mixture of $\text{Ga}_2\text{O}_3(\text{Gd}_2\text{O}_3)$.¹ Recently, we have discovered^{2,3} an epitaxial *single-crystal* Gd_2O_3 film as another excellent candidate for the GaAs(100) surface passivation.⁴ In this paper, we focus on the structural studies of Gd_2O_3 films using single-crystal x-ray diffraction.

II. EXPERIMENT

A triple-axes, four-circle goniometer and a 12-kW rotating anode x-ray source are used in our study of the reciprocal space. A pair of flat graphite crystals are used to monochromatize and analyze the Cu $K\alpha$ x-ray beam, with a resolution of 0.01 Å^{-1} along the longitudinal and 0.005 Å^{-1} along the transverse directions, respectively. The low resolution is chosen intentionally in order to increase the sensitivity to very thin films and make the search in reciprocal space less tedious. The distinct advantages of the triple-axes geometry are the significantly improved separation of θ and 2θ components and the resulting simplification of the data analysis. In a more widely utilized double-crystal geometry, θ resolution is typically about a degree wide, which can cause significant misinterpretations when the films exhibit simultaneously true mosaic features like dislocation caused broadening, layer tilts, and a distribution of layer spacings.

Measurements reported here were carried out in ambient air, where there was no measurable film degradation, in agreement with earlier studies.³

III. RESULTS

In the single-crystal geometry scans were first carried out along the surface normal direction. Here, a broad peak near $2\theta=47.5^\circ$ was identified in 185-, 45-, 25-, and 18-Å-thick Gd_2O_3 films, as shown in Fig. 1. The intensity of this diffraction peak increased while the peak widths decreased with the film thickness, suggesting that it was originating from the epitaxial film. In addition, the peak position shifted towards larger diffraction angles for thicker films, typical to a strain relaxation in the film. All these features were typical characteristics of a strained layer epitaxial film growth. The peak widths in these 2θ - θ scans are a direct measure of the inverse correlation lengths perpendicular to the surface. In a defect-free unstrained epitaxial film, this correlation length corresponds to the film thickness, and the peaks broadened only by the finite-size effect. In a strained and/or defective film, however, a distribution of layer spacings may introduce an additional peak broadening. A separation of the strain-caused broadening and the finite-size caused broadening is often very difficult, especially for thin films with low count rates and only few accessible Bragg peaks. A careful analysis of the intensity distribution around a few diffraction peaks in reciprocal space, however, is often sufficient to extract substantial structural information.

The layer spacing, as determined from the position of the peak near $2\theta=47.5^\circ$, decreases from 2.015 to 1.914 Å, with increasing film thickness. This change in layer spacing indicates a 5.5% strain relaxation in the film, as shown in Fig. 2(a). Here the strain assumes a zero value at the bulk layer spacing of 1.911 Å or (440) of α - Gd_2O_3 , as we will explain later. The widths of the peaks in Fig. 1 are plotted in Fig. 2(b). The 18-Å film exhibits a defect-free region of about 9 Å. The 25-Å film gives a 26-Å correlation length, meaning an essentially defect-free film, while 45- and 185-Å films exhibit 34- and 122-Å correlation lengths, respectively.

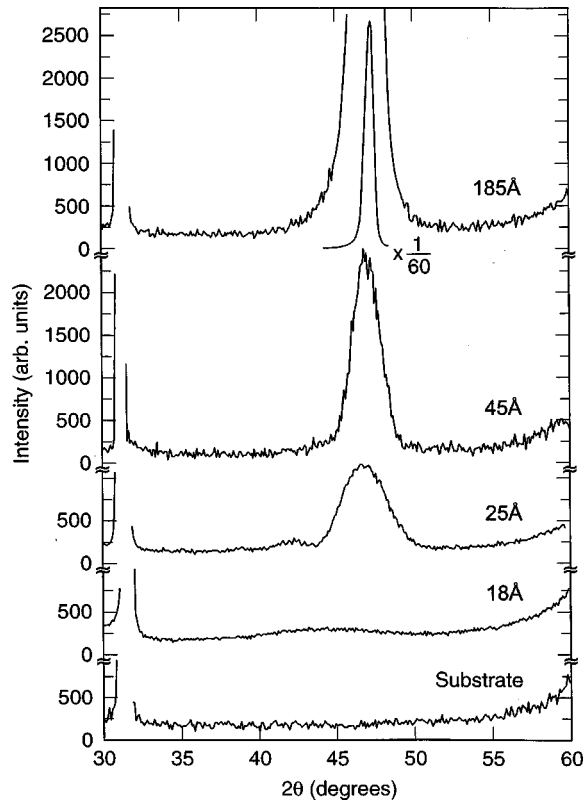


FIG. 1. Reciprocal space scans taken along the surface normal, GaAs(001) direction in four different thickness Gd_2O_3 film samples: 185, 45, 25, and 18 Å, and for the substrate as a background reference.

The θ -rocking or mosaic scans of these peaks at their maximum 2θ positions reveal important information about the nature of defects in the film. A film with defect-free atomic layers, perfectly aligned with the substrate layers yields a sharp peak width identical to that of the substrate peaks, limited by the instrument resolution. The presence of defects, like misfit dislocations, introduces a pronounced mosaic broadening. Figure 3 shows the mosaic scans of these four different films. The 18-Å film shows a single sharp peak with a width of full width at half maximum (FWHM) = 0.39° , which is slightly above the instrumental resolution of 0.25° , while the 25-Å film displays a sharp peak (FWHM = 0.36°) superimposed on a broader peak. For thicker films (45- and 185-Å films), the sharp component disappears, but the broad component persists. The broad component has a width of 3.8° when it first appears in the 25-Å film, but gets narrower with increasing thickness; 3.25° and 1.82° for 45- and 185-Å films, respectively. This we interpret as a fully strained epitaxial growth for the film with a thickness not exceeding 18–25 Å. The broad peak is associated with misfit dislocations, and its width results from the strain fields that exist around individual dislocations. This strain field decays rapidly with distance. It is therefore natural to expect that the thinner films will be most affected since all atoms would experience this strain field in some form. As thickness increases, misfit dislocations and their strain fields would be buried deep at the interface, and the peak widths would gradually decrease, in agreement with our observations.

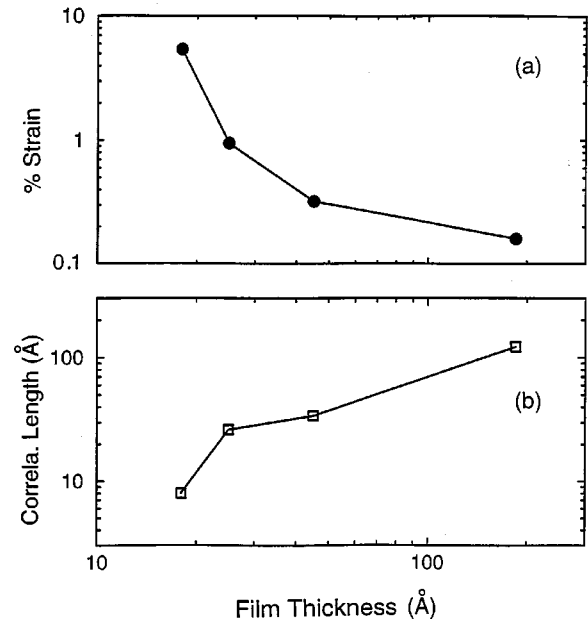


FIG. 2. (a) The layer spacings, which are determined from the peak positions of Fig. 1, decrease with increasing film thickness and approach the bulk $\text{Gd}_2\text{O}_3(440)$ layer spacing of 1.91 Å, indicating a percent strain buildup in the film. (b) Correlation lengths or size of the defect-free regions monotonically increase with thickness.

The level of strain buildup or elastic distortion in the film is directly proportional to the bulk lattice constant difference of the film and the substrate. Thin films can accommodate large elastic strains, but as the thickness increases it becomes energetically more favorable to create misfit dislocations, or discommensurations at the interface that relax the elastic distortion of the film⁵ at a critical thickness. As an example, for the $\text{In}_x\text{Ga}_{1-x}\text{As}/\text{GaAs}(100)$ system the critical thickness varies from 10 to 1000 Å for a strain of 0.07–0.003. These empirical values are in good agreement with the theory.⁶ The measured strain in our 18-Å film is about 0.06, from direct comparison of the peak positions of the 18- and 185-Å films shown in Fig. 1. Here, we assume that the 185-Å film is fully relaxed and assumes the bulk structure of a cubic phase as we will identify next. Interestingly, our assigned critical thickness value in the range 18–25 Å qualitatively agrees with the one found for the $\text{In}_x\text{Ga}_{1-x}\text{As}/\text{GaAs}(100)$ system.

In order to associate the film diffraction peak in Fig. 1 with a particular structure, we examined all known Gd_2O_3 structures that are monoclinic, hexagonal, and cubic structures. For the peak position, we found a good agreement with the (440) peak of the $\alpha\text{-Gd}_2\text{O}_3$ cubic structure.^{7,8} The measured lattice constant of 10.83 Å agreed well with the bulk form of this cubic phase which has a 10.813-Å lattice constant, belongs to the space group $Ia\bar{3}$, and is an isomorph of the Mn_2O_3 structure. This assignment fixed the [110] direction of the film parallel to the surface normal, or [001] direction of the GaAs substrate. In order to find the relative in-plane orientation, we searched for {222} strong reflections of the film on a cone centered around the [110] Gd_2O_3 axis or [001] GaAs axis, i.e., $360^\circ \phi$ scan with a $35.264^\circ \chi$ tilt (the angle between film [111] and [110]). As expected, this scan revealed two {222} peaks at 0° and $180^\circ \phi$

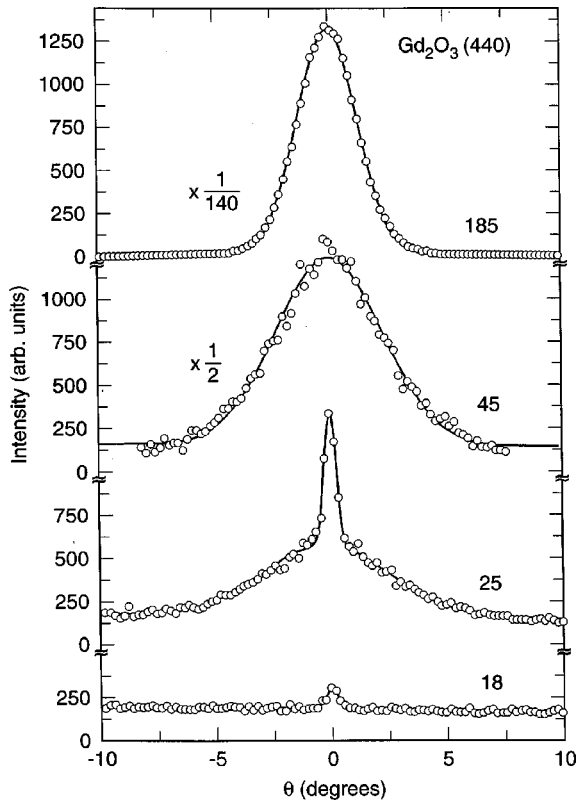


FIG. 3. Mosaic or θ scans for the four different thicknesses Gd_2O_3 film samples find two distinct peak shapes coexisting near 25 Å thickness, a clear indication of strain relaxation through misfit dislocations.

angle at the right lattice spacing. This established an in-plane epitaxial relationship as $[001]_{Gd_2O_3} // [011]_{GaAs}$ and $[\bar{1}10]_{Gd_2O_3} // [01\bar{1}]_{GaAs}$. Figure 4 shows this cone scan. With the twofold $[110]$ film axis aligned along the substrate four-fold axis, epitaxial films were expected to satisfy epitaxial conditions in two degenerate orientations. Interestingly, the Gd_2O_3 films, however, were only growing in one of the two possible orientations with no trace of the other orientation.

We have also carried out scans along all the major zone axes, and searched for peaks that belonged to a second phase. These included specific lattice spacing searches that be-

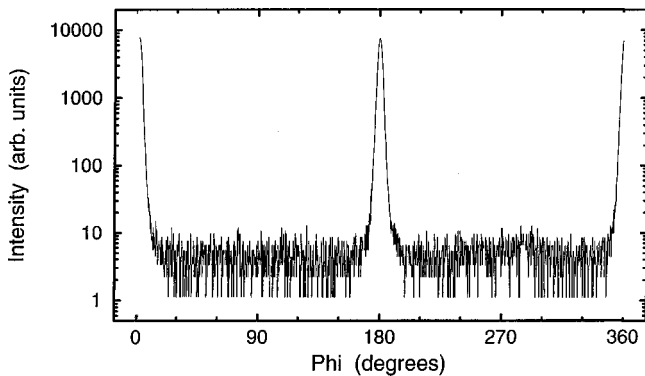


FIG. 4. The $360^\circ \phi$ scan of the 185 Å finds only one pair of $\{222\}$ peaks for the Gd_2O_3 film indicating a single-crystal growth.

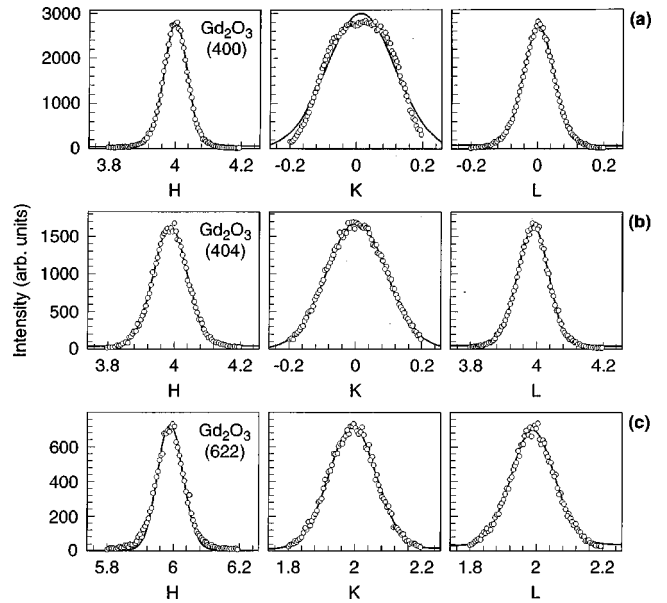


FIG. 5. The measured diffraction peaks of the α - Gd_2O_3 phase. H, K, L refers to the reciprocal lattice of this phase.

longed to the monoclinic and the hexagonal phases. We could not find any evidence for any phase formation other than the cubic phase, in agreement with our *in situ* reflection high-energy electron diffraction observations.^{2,3} We next searched for other peaks that belong to the cubic α phase. All the peaks measured were at their predicted positions. Figure 5 shows some of these major diffraction peaks in reciprocal space where $H, K,$ and L refer to the Gd_2O_3 indices. The measured peak intensities of these peaks are tabulated in Table I, and are compared to values taken from the powder diffraction files. Remarkably, the measured intensity values agreed well with the ones listed for the cubic phase. Observed small deviations in some of the intensities remain within our measurement statistics and analysis errors, considering that no geometrical corrections were made to our data due to the sample geometry. This approximation only

TABLE I. The measured diffraction peak Miller indices and intensities of the 185-Å-thick Gd_2O_3 film. Measured intensities are only corrected for the multiplicity factor. The measured values belong to the bulk phase and are taken from the powder diffraction files file references.

HKL	11-604	12-797	43-1014	Measured
211	10	12	5	7
222	100	100	100	100
321		2	1	2
400	35	35	32	29
411		6	3	5
420		2	1	2
332	5	6	2	4
422		2	<1	0.6
431	10	8	4	9
521		2	1	2
440	40	40	35	34

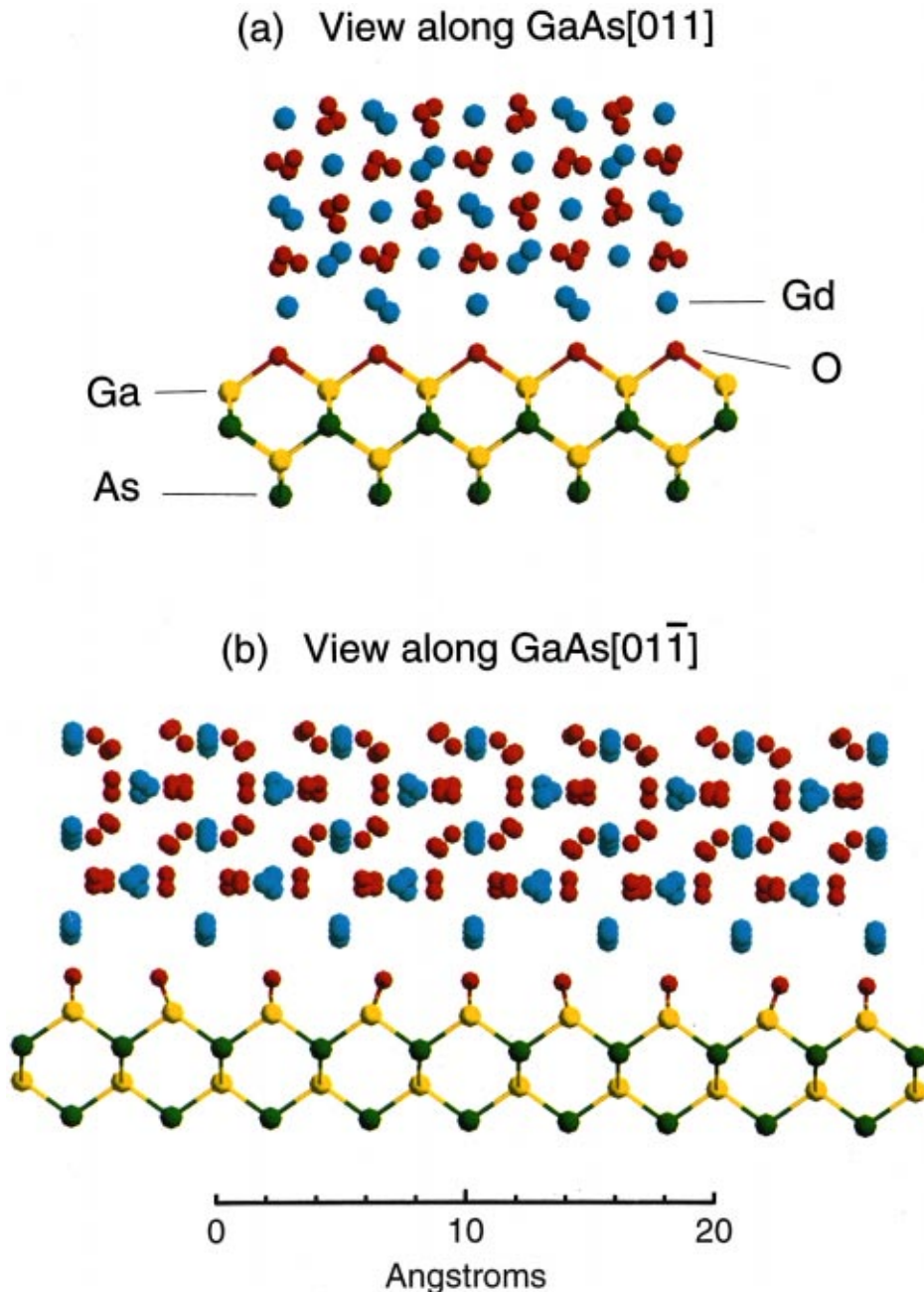


FIG. 6. (Color) A possible structure model for the Gd_2O_3 epitaxial film growth on the GaAs(001) surface, viewed along the two primary axes. The growth may initiate by the substitution of the As sites by the O atoms. The single-crystalline twofold symmetric growth on a fourfold symmetric GaAs(100) surface can be explained by the preference of the one that primarily bends the oxygen bonds at the interface rather than stretching them.

remains valid within a range of diffraction angles where the sampling volume does not vary significantly.

IV. DISCUSSION

The cubic α phase of Gd_2O_3 has a large unit cell $a = 10.79 \text{ \AA}$ compared to that of the GaAs $a = 5.653 \text{ \AA}$. As shown in Fig. 6, the lattice matching conditions of the epitaxial growth are satisfied over unusually long lengths at the interface. In one direction [011] of GaAs, it takes about 32.58 \AA (with a +1.9% lattice mismatch), and in another, [01 $\bar{1}$] GaAs direction, it takes about 15.35 \AA (with a -3.9% lattice mismatch) to match the unit cells. The observed 5.5% strain buildup in thin films, measured from the film layer spacing (Fig. 2), is unusually large, and cannot be explained by the observed in-plane lattice mismatch values alone. This is a clue that something unusual is taking place at the inter-

face, which is causing this additional distortion in the size and shape of the equilibrium unit cell. This can be caused by a grossly distorted covalent bonding of atoms at the interface.

It is unlikely that interatomic forces acting over 32.58- and 15.35- \AA distances can be responsible for this supercell epitaxy. This is especially true during the initial stages of the growth, when there are too few Gd and O atoms on the surface even to complete a single unit cell. Since the epitaxial growth starts with nucleation at many different sites across the substrate surface, the overall film growth will not be coherent but will compose of single-crystalline regions that have a shifted phase relationship with respect to each other, forming so-called antiphase boundaries in between. As the unit-cell matching length increases, the number of possible nucleation sites or density of antiphase boundaries is expected to increase in proportion. In addition to this large

degree of degeneracy for possible nucleation sites, in the $\text{Gd}_2\text{O}_3/\text{GaAs}(100)$ case there is a rotational degeneracy; the (110) twofold planes of the film, in principal can satisfy the same epitaxial relations in two different orientations on the fourfold symmetric (100) planes of the substrate. Remarkably, the system chooses only one orientation, and grows with a high structural perfection.

In the case of molecular beam epitaxy growth of II-VI compounds on GaAs, the interface chemistry can be successfully studied by the consideration of valence electrons of the surface compounds. Typically, the excess of valence electrons can lead to a distortion of the tetrahedral configuration of the bonding at the interface, and can change the number of bonds from four to three or two. In the tetrahedral bond configuration, GaAs has four valence electrons per atom. In the Ga_2O_3 sesquioxide, the Ga atom contributes three valence electrons and the O atom contributes six electrons to a Ga-O bond. This results in an extra electron, which makes the tetrahedral configuration in Ga_2O_3 unstable. A tetrahedral lattice, however, can still be formed if one third of Ga sites are left vacant. With these vacancies included the valence electron counting assigns $(3 \times 2 + 6 \times 3)/6 = 4$ electrons per site on the average.⁹ The growth behavior of another trivalent sesquioxide like Gd_2O_3 is expected to be similar to that of the Ga_2O_3 growth. The first few layers may have no difficulty in continuing the growth of the substrate tetrahedral lattice, by leaving some Gd sites vacant. But since the equilibrium α phase has a nontetrahedral coordination, a transition to this structure will introduce a partial disorder. This is expected to be prevalent especially for very thin layers, which agrees with our observations. The integrated intensities of Gd_2O_3 (440) for the 18-Å film fall significantly short of the 25-Å film as can be seen in Figs. 1 and 3. This can be attributed to a film with a large volume fraction in a disordered state. The presence of a disordered transition region may also partially relieve some of the strain caused by the mismatch.

One reasonable explanation for this preferred alignment along only one of the two possible orientations during the single-crystal epitaxial growth would be a chemistry-enforced local ordering that imposes a deterministic growth by strongly favoring certain binding sites. A close look at the structure of the interface and the atomic decoration of the unit cells in Fig. 6 reveals that, indeed there is such a short-range order at the interface. Along the $[01\bar{1}]$ short supercell direction, the substrate and Gd_2O_3 film consist of rows of atoms with similar spacings. Our x-ray measurements determine the structure of the growing film, the substrate and their relative orientations, but does not reveal the atomic positions at the interface. In order to be able to construct the interface structure and understand the importance of these rows, let us examine some bond strengths. Among the Gibbs free energy of formations for all possible pairs in Ga, As, Gd, and O, Gd_2O_3 is the strongest, followed by Ga_2O_3 , and the rest of all possible binaries are negligible in comparison. The lattice energy of Ga_2O_3 is 15 590 kJ/mol, the second largest lattice energy known, surpassed only by Al_2O_3 lattice energy of 15 916 kJ/mol, while the lattice energy of Gd_2O_3 is 12 996 kJ/mol. Based on this information, the epitaxial growth should preferentially start first with a layer of oxygen atoms bonding to a Ga terminated surface. The oxygen atoms in

this layer occupy the same positions as the As atoms would, as governed by the directional or the covalent nature of the bonding in GaAs substrate. This immediately explains the similarity of the rows of atoms between the two lattices. Indeed, oxygen atoms in As sites at the interface are shared by the two lattices, would enforce this local order, and facilitate the single-crystal growth. If the GaAs surface was initially As terminated, oxygen would directly replace and substitute As, liberating it from the interface, and this extra layer of As would either dissolve in the growing film, segregate to the surface, or would sublimate, depending on the growth conditions. High mobility and volatility of As is a well-known fact, as has been observed in $\text{Ga}_{1-x}\text{In}_x\text{P}$ growth on GaAs.¹⁰

Once the positions of the As atoms at the interface are assigned to that of the O atoms, the puzzle of single-crystal growth is essentially solved. This will fix the positions of the oxygen atoms in the Gd_2O_3 lattice growing on this template. The (110) plane of the bulk phase of the α - Gd_2O_3 has a similar configuration for the oxygen atoms. So far, we have explained the interface structure and the epitaxial growth but have not explained why the system chooses only one orientation out of two possible ones for the epitaxial growth. For this, we have to look at the second layer of atoms and beyond. Here, Gd atoms form the same rows as the O atoms, but now there are one quarter less Gd atoms compared to the O atoms. As a result, oxygen atoms are rearranged along the rows to accommodate these missing Gd atoms. This significantly distorts the bonds and displace the O atoms from their tetrahedral sites toward their equilibrium positions in the bulk Gd_2O_3 structure. Since every O atom is bonded to two Ga atoms at the interface, its displacement would involve bond stretching and bond bending. The two degenerate growth orientations, therefore, distinguish themselves as being either predominantly bond bending or bond stretching. Since displacement of oxygen atoms along the rows shown would involve primarily bond bending, this should be energetically favored over the alternative degenerate orientation that primarily favors stretched Ga-O bonds, as shown in Fig. 6.

The Gd_2O_3 epitaxial films on GaAs(100) are also interesting for studying the dislocation formation. These films experience very different forces along the two in-plane directions. Along the $[01\bar{1}]$ GaAs direction it is under a large tensile strain (-3.9%), while in the orthogonal direction it experiences a compressive strain (1.9%). If strain relaxation takes place through the creation of misfit dislocations, these dislocations are expected to be uniaxial. In a likely scenario, uniaxial dislocations may form separately in both the substrate and the films but substrate ones would be orthogonal to film dislocations. These important and interesting issues may find answers through further studies of this system by high-resolution electron and high-resolution x-ray diffraction experiments.

ACKNOWLEDGMENTS

We thank D. Murphy, R. Tung and R. M. Fleming for valuable discussions.

- ¹M. Hong, M. Passlack, J. P. Mannaerts, J. Kwo, S. N. G. Chu, N. Moriya, S. Y. Hou, and V. J. Fratello, *J. Vac. Sci. Technol. B* **14**, 2297 (1996).
- ²J. Kwo, M. Hong, A. R. Kortan, D. W. Murphy, J. P. Mannaerts, A. M. Sergent, Y. C. Wang, and K. C. Hsieh, *Mater. Res. Soc.* **673**, 57 (1999).
- ³M. Hong, J. Kwo, A. R. Kortan, J. P. Mannaerts, and A. M. Sergent, *Science* **283**, 1897 (1999).
- ⁴T. Hashizume, K. Ikeya, M. Mutoh, and H. Hasegawa, *Appl. Surf. Sci.* **123**, 599 (1998).
- ⁵R. Hall and J. C. Bean, in *Strained-Layer Superlattices: Materials Science and Technology*, edited by T. P. Pearsall (Academic, New York, 1991), p. 1.
- ⁶I. J. Fritz, S. T. Picraux, L. R. Dawson, T. J. Drummond, W. D. Laidig, and N. G. Anderson, *Appl. Phys. Lett.* **46**, 967 (1985).
- ⁷D. Grier and G. McCarthy (unpublished).
- ⁸S. Geller, *Acta Crystallogr., Sect. B: Struct. Crystallogr. Cryst. Chem.* **B27**, 821 (1971).
- ⁹Yu. G. Sidorov, S. A. Dvoretzky, M. V. Yakushev, N. N. Mikhailov, V. S. Varavin, and V. I. Liberman, *Thin Solid Films* **306**, 253 (1997).
- ¹⁰O. Dehaese, X. Wallart, O. Schuler, and F. Mollot, *Jpn. J. Appl. Phys., Part 1* **36**, 6620 (1997).